Numerical Analysis of Electromagnetically Induced Heating and Bioheat Transfer for Magnetic Fluid Hyperthermia

Lei Wu[1], Jingjing Cheng[2], Wenzhong Liu[2], and Xiangguang Chen[1]

[1]School of Chemical Engineering and Environment, Beijing Institute of Technology, Beijing 100081, China
[2]School of Automation, Huazhong University of Science and Technology, Wuhan 430074, China

In this paper, we study the computational modeling of electromagnetically induced heating in magnetic fluid hyperthermia. Owing to the Brownian rotation and Neel relaxation of induced magnetic moments, ferrofluids can generate heat when exposed to an alternating current magnetic field. To destroy all tumors cells while preventing deleterious physiological responses, input parameters such as the frequency and intensity of magnetic fields and the complex susceptibility of ferrofluids should be determined precisely. In this paper, a solution to Maxwell's equation for a model of a tumor and its neighboring tissues are coupled as input to Penne's bioheat equation. Both sets of equations are solved using the finite element analysis method with perfectly matched layers for isothermal boundary conditions in COMSOL. We use a bilayered spherical model with blood perfusion and metabolism to simulate the temperature distribution in tumor regions during hyperthermia therapy. Power density due to electromagnetic field simulation serves as input to the bioheat transfer equation and determines the heat generated by the ferrofluids. The obtained results indicate that tumor regions are heated without adversely affecting healthy regions.

***Index Terms*— AC magnetic field, bilayered spherical mode, bioheat equation, finite element analysis (FEA), magnetic fluid hyperthermia.**

I. Introduction

MAGNETIC fluid hyperthermia (MFH) is a promising treatment method for cancer lesions and can be used as a complement to chemotherapy or for the direct ablation of tumors by heat treatment [1]. During hyperthermia therapy, a sustained temperature between 40 °C and 45 °C within a tumor for a defined period would induce cell apoptosis without damaging surrounding healthy tissues.

The critical problem of hyperthermia is the direct provision of a well-controlled and localized heat source to the tumor tissue. Among the hyperthermia methods presented in [2] and [3], MFH is considered one of the best treatment approaches because of its uniform heating effect and deep penetration depth. In MFH, the heat effect is due to an alternating current (ac) magnetic field of biocompatible and biodegradable nanoparticles injected inside the tumor; the heat effect should be uniform in the treatment area [4]. Given that these particles are nanoscale elements, the energy deposition in cancer cells are extremely localized.

MFH is a complicated multiphysics problem which is covered by two partially independent solutions: one solution for the magnetic field equation and the other for the heat transfer equation [5], [6]. In the current paper, a complete mathematical model of MFH is proposed and analyzed to simulate heat generation and transfer during magnetic hyperthermia. To estimate the temperature distribution in tumor regions and surrounding normal tissues, both electromagnetic and thermal problems are solved using the finite element analysis (FEA) method in COMSOL. Power density is derived from electromagnetic field simulation and is computed as the input of Penne's bioheat equation. The obtained results indicate that cancerous tissue can be heated sufficiently without damaging healthy regions.

Manuscript received March 7, 2014; revised May 1, 2014; accepted September 12, 2014. Date of current version March 20, 2015. Corresponding author: J. Cheng (e-mail: frankiefox@163.com).

Color versions of one or more of the figures in this paper are available online at http://ieeexplore.ieee.org.

Digital Object Identifier 10.1109/TMAG.2014.2358268

II. Theory and Method

The heating mechanism for magnetic nanoparticle fluids has been detailed by Rosensweig [7] by using the Debye model for dielectric dispersion in polar fluids. When a time-varying magnetic field H_0 is applied to ferrofluid, nanoparticles and their magnetic moments rotate to align with the changing field [8]. The rotation of the particle in the viscous medium (i.e., Brownian rotation) and the rotation of magnetic moments (i.e., Neel relaxation) are the dominant means of power dissipation caused by friction [9]. The characteristic Brown and Neel relaxation times are expressed as follows:

$$\tau_N = \tau_0 \exp\left(\frac{KV}{kT}\right),\ \tau_B = \frac{3\eta V_H}{kT} \tag{1}$$

where η is the dynamic viscosity of a medium wherein particles are suspended, K is the effective anisotropy constant, kT is the thermal energy, V_H is the hydrodynamic particle volume, V is the volume of the magnetic core, and τ_0 is the attempt time, which is approximately 10^{-9} s. The volumetric heating power (P) caused by nanoparticle relaxation can be evaluated as follows:

$$P = \mu_0 f H_0^2 \pi \chi'' \tag{2}$$

where μ_0 is the magnetic permeability of the vacuum, f is the frequency of the ac magnetic field, H_0 is the magnitude of the applied magnetic field, and χ'' is the imaginary part of the complex magnetic susceptibility. The latter is a function of the Langevin parameter and magnetic field frequency

$$\chi'' = \chi_0 \frac{2\pi f \tau_{\text{eff}}}{1 + (2\pi f \tau_{\text{eff}})^2} \tag{3}$$

where τ_{eff} is the relaxation time of nanoparticles due to τ_N and τ_B such that $\tau_{\text{eff}}^{-1} = \tau_N^{-1} + \tau_B^{-1}$ and χ_0, the static susceptibility is represented as follows:

$$\chi_0 = \chi_i \frac{3}{\xi}\left(\coth \xi - \frac{1}{\xi}\right) \tag{4}$$

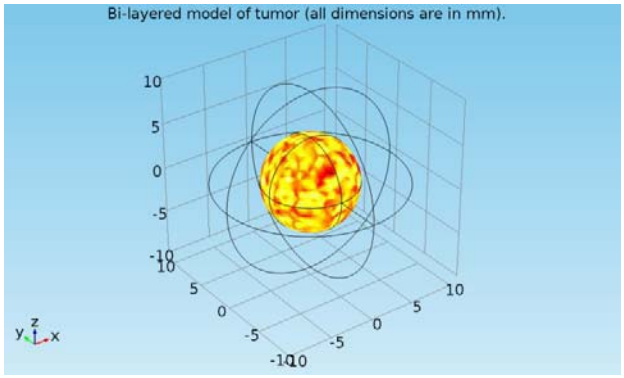

(a)

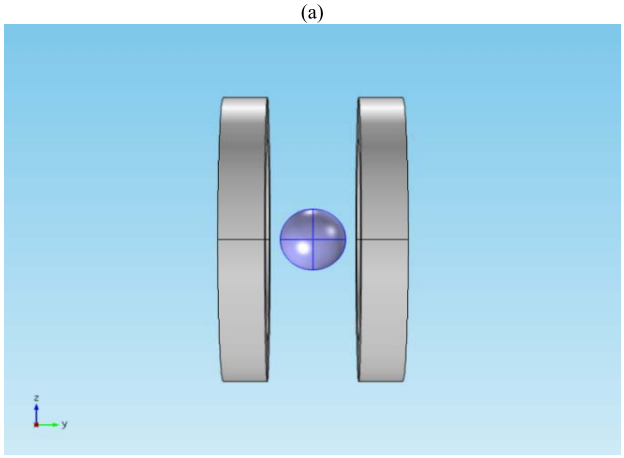

(b)

Fig. 1. (a) Bilayered model of a tumor. (b) Helmholtz coils, including a central composite region of tumor tissue and magnetic nanoparticle fluid.

where ξ, the Langevin parameter, and the initial susceptibility χ_i are expressed as follows:

$$\xi = \frac{\mu_0 M_d \mathrm{HV}}{kT}, \quad \chi_i = \frac{\mu_0 \phi M_d^2 V}{3kT} \tag{5}$$

where M_d is the domain magnetization of the magnetic nanoparticle.

The computed power dissipation are then substituted as a heat source into Penne's bioheat equation to calculate the temperature distribution of tumors and its surrounding normal tissues [10]. The bioheat equation, including the effects of blood perfusion and metabolic heating, is represented by the following:

$$\rho c \frac{\partial T}{\partial t} = \nabla \cdot (k \nabla T) + \rho_b c_b \omega (T - T_b) + Q_m + P \tag{6}$$

where ρ is the tissue density, c is the specific heat for the tissue, k is the thermal conductivity of the tissue, ρ_b is the blood density, c_b is the specific heat for blood, ω is the blood perfusion rate, T_b is blood temperature, Q_m is metabolic heating, and P is the heat added to the system from a source, such as the heating caused by the ferrofluid in an ac field.

III. Model and Materials

To simplify this problem, we ass ume that the tumor is spherical with radius $r = 5$ mm and that the surrounding normal tissue is a large concentric sphere with radius $a = 10$ mm [Fig. 1(a)]. To generate a uniform field, the current version of the model uses Helmholtz coils to provide the ac magnetic field.

TABLE I
Material Properties for Tumor/Ferrofluid Composite Region

Tissue name	Tumor tissue	Magnetic Ferrofluid	Composite region
Specific heat capacity ($J \cdot kg^{-1} \cdot K^{-1}$)	3500	4000	3501.5
Thermal conductivity ($W \cdot m^{-1} \cdot K^{-1}$)	0.55	40	0.552
Density ($kg \cdot m^{-3}$)	1060	5180	1070.4

A Helmholtz pair consisting of two identical circular coils of radius r are placed symmetrically on each side of the experimental area along a common axis and are separated by distance L. Each coil contains N turns of wires and carries equal electrical currents that flow in the same direction. The origin of a coordinate system is centered on the axis at the middle of the coil centers. The axial component of the magnetic flux density at a distance from the origin is expressed as follows:

$$B = \frac{\mu_0 \mathrm{NI} r^2}{2\left[r^2 + \left(\frac{d}{2} + x\right)\right]^{3/2}} + \frac{\mu_0 \mathrm{NI} r^2}{2\left[r^2 + \left(\frac{d}{2} - x\right)\right]^{3/2}} \tag{7}$$

where μ_0 is called the permeability of free space.

Homogeneity causes all thermodynamic parameters in the tissues to be the same. We assume homogeneity within the target region. The mean value of specific heat, density, and electrical conductivity for cancerous tissues with embedded nanoparticles can be approximated by a serial arrangement of the two materials with two volume proportions

$$\rho_{\text{composite}} = (1 - v)\rho_{\text{tumor}} + v\rho_{\text{ferrofluid}} \tag{8}$$

$$c_{\text{composite}} = (1 - v)c_{\text{tumor}} + vc_{\text{ferrofluid}} \tag{9}$$

$$\frac{1}{k_{\text{composite}}} = \frac{(1 - v)}{k_{\text{tumor}}} + \frac{v}{k_{\text{ferrofluid}}} \tag{10}$$

where v is the volume fraction of magnetite nanoparticles in the tumor region. A total of 10 mg Fe/g of tumor corresponds to a volume fraction of $v = 0.003$. This dosage is the typical dosage reported in clinical studies [11]. The tumor and ferrofluid material properties used in this paper to determine the composite values for calculation are provided in Table I. The thermal properties and densities for tumor and magnetic ferrofluid were obtained from [12]–[14].

IV. Results and Discussion

In magnetic nanoparticle therapy, heat is generated by a time-varying magnetic field H that causes the rotation of nanoparticles and their magnetic moments in the biological fluid. Maxwell equations in magnetic problems are computed according to the appropriate boundary, whereas Penne's bioheat equation in thermal problems is calculated by considering blood perfusion. In this paper, both electromagnetic and thermal problems are solved by FEA.

A. Magnetic Field Uniformity

The uniformity of a magnetic field is considered as a prerequisite for uniform temperature distribution in a target region.

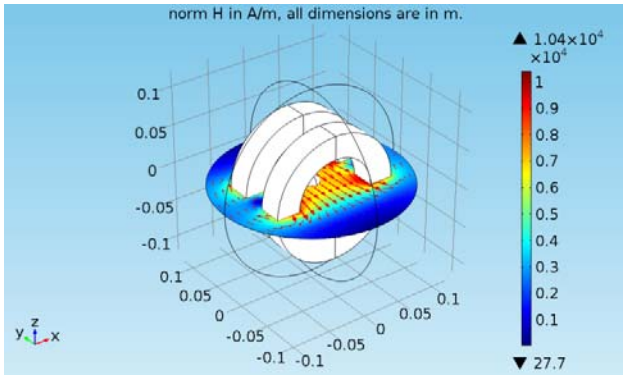

Fig. 2. 3-D plots of magnetic field distribution in tumor regions between Helmholtz coils. norm(H) is the norm of magnetic field vector.

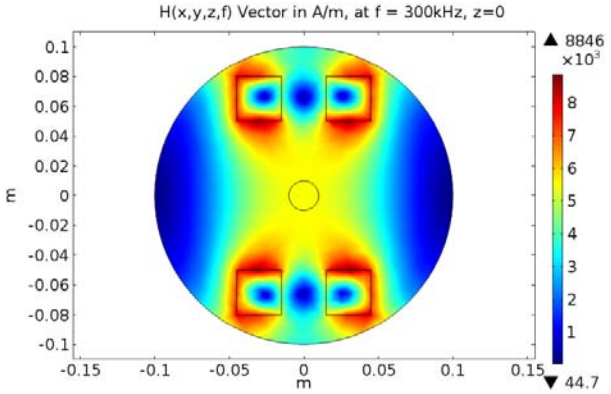

Fig. 3. 2-D surface plot for magnetic field at 300 kHz to illustrate field uniformity in the x–y plane in a central slice.

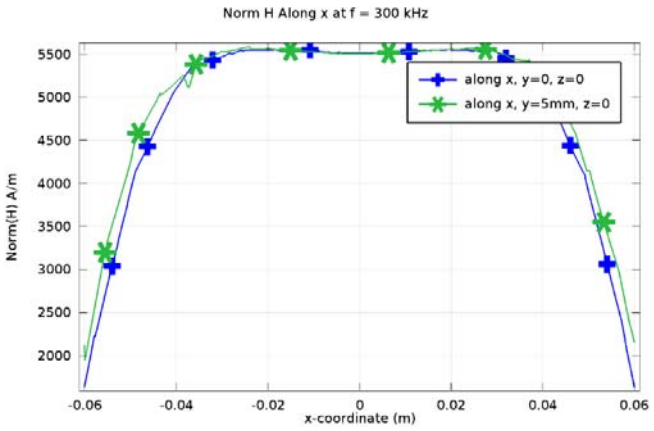

Fig. 4. norm(H) at 300 kHz and a maximum applied magnitude of 5518 A/m along the x-axis. norm(H) is uniform within 5% at 5 mm for the origin along the y-axis.

Thus, calculations are first performed to verify the uniformity of the magnetic field caused by Helmholtz coils.

In our calculations, the ac in the coils is 5 A at 300 kHz, thus leading to an applied field of 5518 A/m at the origin points. Figs. 2 and 3 show the magnetic field distribution in 3-D and 2-D, respectively. Fig. 4 shows the norm(H) along the x-axis at $y = 0, z = 0$ (blue line) and $y = 5$ mm, $z = 0$ (green line). Figs. 2–4 show that the applied field is uniform within the region of interest for the field strengths and frequency of use for MFH. For hyperthermia in cancer

TABLE II
PRAMETERS FOR THE CALCULATION OF POWER DISSIPATION

Parameter	Description	Value
R	Magnetic nanoparticle radius	9.5×10^{-9} m
f	Frequency	300 kHz
H_0	Field Strength	5518 A / m
μ_0	Permeability in vacuum	$4\pi\times10^{-7}$ Tm / A
k	Boltzman constant	1.38×10^{23} J / K
K	Effective anisotropy constant	1.0×10^{4} J / m^3
V_H	Hydrodynamic particle volume	5.0805×10^{-22} m^3
τ_0	Attempt time	10^{-9} s
η	Dynamic viscosity	1×10^{-3} kg / m / s
ϕ	Volume fraction solid	0.071
M_d	Domain magnetization	446 kA / m

TABLE III
PROPERTIES OF BLOOD IN TUMOR AND NORMAL TISSUE

Tissue name	Blood in tumor	Blood in normal tissue	Normal tissue
Specific heat capacity ($J\cdot kg^{-1}\cdot K^{-1}$)	4180	4180	2300
Perfusion Rate ($1/s$)	1.39×10^{-2}	6.67×10^{-3}	--
Density ($kg\cdot m^{-3}$)	1000	1000	980
Thermal conductivity ($W\cdot m^{-1}\cdot K^{-1}$)	0.512	0.512	0.25

treatment, the treatment temperature should be within the acceptable range in clinical practice. For our model frequency, the magnetic field strength is 5518 A/m. The parameters used to calculate the heat dissipation of the nanoparticles are adapted from [15] and [16] and gathered in Table II.

B. Bioheat Transfer

In the thermal calculations, the initial temperature is set to 37 °C for all tissue layers. The characteristic coefficients are independent of the position within the region. This model enables the study of nonlocalized transient temperature behavior in tissues wherein fluctuation in the heat flux and temperature extends throughout many physiological regions where perfusion, density, specific heat, and metabolic heat generation vary. The properties of normal tissue and blood both in the tumor and healthy tissue in this model are listed in Table III [13].

The temperature distribution in the tumor region and healthy region is important in hyperthermia. In this research, we analyze the temperature at the center region of the tumor tissue and monitor the increase in heat in the healthy tissue. In this model, the temperature distribution reaches a steady state after 200 s. Fig. 5 shows the temperature distribution in the target region. Given the isothermal boundary condition, the edge of normal tissues is at a constant temperature of 37 °C. The maximum temperature, that is, 43.47 °C, appears at the

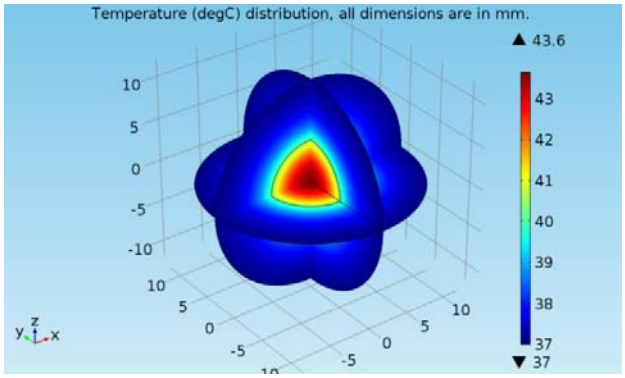

Fig. 5. 3-D plots of temperature distribution in the tumor and normal tissue.

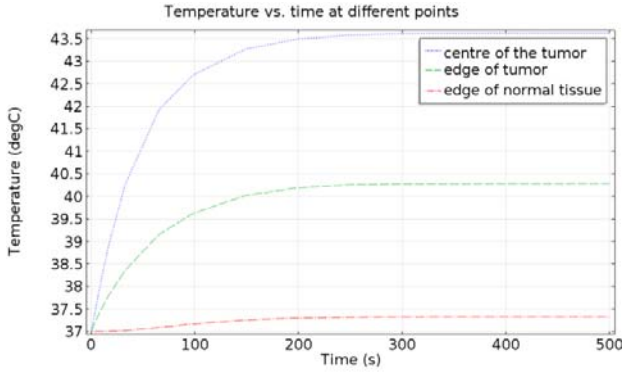

Fig. 6. Temperature versus time for heating at the center of the tumor and edges of the tumor and healthy tissue.

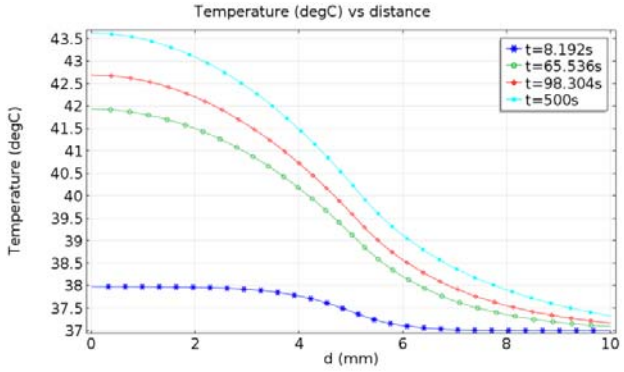

Fig. 7. Temperature distribution as a function of the distance from the center of the tumor for different exposure times.

center of the tumor region where nanoparticles are evenly distributed. The temperature in the center region is maintained in the range of 40 °C–45 °C, which is sufficient for hyperthermia cancer therapy. The temperature of the healthy region without heat generation is below 40 °C. Minimal damage is observed in the healthy region. Besides, eddy-current-induced heating of small magnetic particles is negligibly small compared with magnetic losses.

The results for temperature versus time are shown in Fig. 6. Material properties and perfusion rates have been detailed in Tables I and III. After 200 s of excitation, the temperature at the center and edge of the tumor reach a steady value, whereas the temperature at the edge of the normal tissue remains at 37 °C during all therapy processes. Fig. 7 shows that the temperature decreases with increasing distance from the center at different exposure times.

V. Conclusion

This paper has proposed a bilayered spherical mode of MFH with a magnetic field generated by Helmholtz coils to establish a complete mathematical description and multiphysics simulation of MFH. The FEA method has been implemented to solve a coupled 3-D electromagnetic thermal problem. A marked increase is observed in the tissue temperature near the center of the tumor region, and a degree of temperature distribution uniformity is achieved. The obtained results indicate that cancerous tissue is heated sufficiently without adversely affecting normal tissues.

References

[1] L. Rast and J. G. Harrison, "Computational modeling of electromagnetically induced heating of magnetic nanoparticle materials for hyperthermic cancer treatment," *PIERS Online*, vol. 6, pp. 690–694, Jul. 2010.

[2] S. L. Ho, L. Jian, W. Gong, and W. N. Fu, "Design and analysis of a novel targeted magnetic fluid hyperthermia system for tumor treatment," *IEEE Trans. Magn.*, vol. 48, no. 11, pp. 3262–3265, Nov. 2012, doi: 10.1109/TMAG.2012.2195161.

[3] S. Dutz and R. Hergt, "Magnetic nanoparticle heating and heat transfer on a microscale: Basic principles, realities and physical limitations of hyperthermia for tumour therapy," *Int. J. Hyperthermia*, vol. 29, no. 8, pp. 790–800, Dec. 2013.

[4] G. F. Goya, V. Grazú, and M. R. Ibarra, "Magnetic nanoparticles for cancer therapy," *Current Nanosci.*, vol. 4, no. 1, pp. 1–16, Feb. 2008.

[5] A. Candeo and F. Dughiero, "Numerical FEM models for the planning of magnetic induction hyperthermia treatments with nanoparticles," *IEEE Trans. Magn.*, vol. 45, no. 3, pp. 1658–1661, Mar. 2009.

[6] P. Di Barba, F. Dughiero, and E. Sieni, "Magnetic field synthesis in the design of inductors for magnetic fluid hyperthermia," *IEEE Trans. Magn.*, vol. 46, no. 8, pp. 2931–2934, Aug. 2010.

[7] R. E. Rosensweig, "Heating magnetic fluid with alternating magnetic field," *J. Magn. Magn. Mater.*, vol. 252, pp. 370–374, Nov. 2002.

[8] P. Di Barba, F. Dughiero, E. Sieni, and A. Candeo, "Coupled field synthesis in magnetic fluid hyperthermia," *IEEE Trans. Magn.*, vol. 47, no. 5, pp. 914–917, May 2011.

[9] C. L. Ondeck *et al.*, "Theory of magnetic fluid heating with an alternating magnetic field with temperature dependent materials properties for self-regulated heating," *J. Appl. Phys.*, vol. 105, no. 7, pp. 07B324-1–07B324-3, 2009.

[10] S. M. Yacoob and N. S. Hassan, "FDTD analysis of a noninvasive hyperthermia system for brain tumors," *Biomed. Eng. Online*, vol. 11, pp. 1–22, Aug. 2012.

[11] K. Parekh, R. V. Upadhyay, R. V. Mehta, and V. K. Aswal, "Experimental investigation of nearly monodispersed ternary $Mn_{0.5}Zn_{0.5}Fe_2O_4$ magnetic fluid," *Magnetohydrodynamics*, vol. 43, no. 4, pp. 393–399, 2007.

[12] D. Arora, M. Skliar, and R. B. Roemer, "Model-predictive control of hyperthermia treatments," *IEEE Trans. Biomed. Eng.*, vol. 49, no. 7, pp. 629–639, Jul. 2002.

[13] M. Pavel, G. Gradinariu, and A. Stancu, "Study of the optimum dose of ferromagnetic nanoparticles suitable for cancer therapy using MFH," *IEEE Trans. Magn.*, vol. 44, no. 11, pp. 3205–3208, Nov. 2008.

[14] Y. Lv, Z. S. Deng, and J. Lui, "3-D numerical study on the induced heating effects of embedded micro/nanoparticles on human body subject to external medical electromagnetic field," *IEEE Trans. Biomed. Eng.*, vol. 4, no. 4, pp. 284–294, Dec. 2005.

[15] A. Miaskowski and B. Sawicki, "Magnetic fluid hyperthermia modeling based on phantom measurements and realistic breast model," *IEEE Trans. Biomed. Eng.*, vol. 60, no. 7, pp. 1806–1813, Jul. 2013.

[16] R. Hergt, S. Dutz, and M. Zeisberger, "Validity limits of the Néel relaxation model of magnetic nanoparticles for hyperthermia," *Nanotechnology*, vol. 21, no. 1, pp. 015706-1–015706-5, 2010.